Progress In Electromagnetics Research M, Vol. 38, 25–35, 2014

Photonic Analysis of Semiconductor Fibonacci Superlattices: Properties and Applications

Hadi Rahimi*

Abstract—In this paper, we theoretically study the phase treatment of reflected waves in one-dimensional Fibonacci photonic quasicrystals composed of nano-scale fullerene and semiconductor layers. The dependence of the phase shift of reflected waves for TE mode and TM mode on the wavelength and incident angle is calculated by using the theoretical model based on the transfer matrix method in the infrared wavelength region. In the band gaps of supposed structures, it is found that the phase shift of reflected wave changes more slowly than within the transmission band gaps. Furthermore, the phase shift decreases with the incident angle increasing for TE mode, and increases with the incident angle increasing for TM mode. Also, for the supposed structures it is found that there is a band gap which is insensitive to the order of the Fibonacci sequence. These structures open a promising way to fabricate subwavelength tunable phase compensators, very compact wave plates and phase-sensitive interferometry for TE and TM waves.

1. INTRODUCTION

The experimental discovery of quasicrystals [1] has given rise to a sudden breakthrough in the area of solid state physics. The structure of quasicrystals exhibits long-range order or correlations between distant parts, but at the same time there is no underlying periodicity, in the sense that a shifted copy of the crystal never matches exactly the original one. In fact, quasicrystals represent an intermediate stage between random media and periodic crystals, effectively combining both localization properties as a result of short-range disorder and the presence of band gaps due to long-range correlations [2]. The concept of quasiperiodicity was readily transferred to photonic crystals and proved to be of great value for many practical purposes [3, 4]. Photonic quasicrystals are deterministically generated dielectric structures with a non-periodic modulation of the refractive index. In the one-dimensional (1D) case, they can be formed by stacking together dielectric layers of several different types according to the substitutional sequence under investigation (Cantor, Fibonacci, Rudin-Shapiro, Thue-Morse, etc.) [6]. The Fibonacci sequence is of particular importance, since it leads to the existence of two incommensurable periods in the spatial spectrum of the structure. Such behavior is typical of sequences with a so-called pure point spectrum, which makes the Fibonacci sequence truly quasiperiodic, as a consequence of the appearance of Bragg-like peaks in the spatial spectrum [5]. This property has been demonstrated to be very valuable for nonlinear optical applications, such as third harmonic generation [7]. In fact, the latter is a two-stage process, and for each stage different phase matching conditions should be met. The Fibonacci sequence allows to fulfill both of them simultaneously and on the same crystal [8]. Studies of some other aspects of wave propagation in the Fibonacci quasicrystals carried out in Refs. [9–13] have considerably improved our understanding of wave transport in the Fibonacci quasiperiodic structures.

Fullerenes are a form of carbon molecule that is neither graphite nor diamond. They consist of a spherical, ellipsoid, or cylindrical arrangement of dozens of carbon atoms. Fullerenes occur only in small

Received 9 July 2014, Accepted 5 August 2014, Scheduled 13 August 2014
* Corresponding author: Hadi Rahimi (h_rahimi@tabrizu.ac.ir).
The author is with the Physics Department, Islamic Azad University, Shabestar Branch, Shabestar, Iran.

amounts naturally, but several techniques for producing them in greater volumes have been suggested in lab. For the past decade, the chemical and physical properties of fullerenes have been a hot topic in the field of research and development, and are likely to continue to be for a long [14–17]. Recently, fullerenes-60 (C60) have attracted much scientific attention due to their novel optical and electrical properties and potential applications such as alkali metal-doped fullerenes become superconductor, while doped thin films act as a conductor [18–20]. The structural modification of C60 fullerenes is very easy which causes the simplicity of the technological treatment. The electronic and optical properties of C60 fullerenes films can be engineered by modifying the geometry and the degree of conjugation of carbon superstructure. This property of C60 fullerenes can be utilized for the fabrication photonic crystal structures using the fullerenes films. High-quality C60 thin films have been grown on various semiconductor and metal substrates, such as Te [21], Ge [22], GaAs [23], Ag [24] and so on. C60 thin films have almost zero absorption in the wavelength range > 530 nm and near IR region [25]. Also, in this region its dielectric constant has very small dependence on the frequency and can be ignored. Thus being a metallic counter part as well as almost frequency independent dielectric constant and easier fabrication technique it is useful in designing the PC structure [25–29].

In this paper, the feasibility of using C60 fullerene/tellurium (Te), C60 fullerene/germanium (Ge) and C60 fullerene/gallium arsenide (GaAs) nano-scale multilayer films as 1D Fibonacci superlattice structures are theoretically investigated. For TE and TM modes, we study the photonic transmission and phase treatment of EM waves in the supposed structure. The analysis has been done by using theoretical model based on the transfer matrix method (TMM) in the near infrared wavelength region. In the band gaps of structure, it is found that the phase shift of reflected wave changes more slowly than within the transmission band gaps. Furthermore, the phase shift of reflected wave decreases with the incident angle increasing for TE mode, and increases with the incident angle increasing for TM mode. The organization of this paper is as follows: In Section 2, we present the mathematical model describing 1D multilayer structure. The results and discussion are presented in Section 3. Finally, we conclude the paper with Section 4.

2. MODEL AND NUMERICAL METHODS

Quasiperiodic structures, which can be idealized as the experimental realization of a 1D quasicrystal, are composed from the superposition of two (or more) building blocks that are arranged as 1D Fibonacci superlattice structure. The Fibonacci sequence is the oldest example of a quasiperiodic chain. It was developed by Leonardo de Pisa (whose nickname was Fibonacci, which means son of Bonacci) in 1202 as a result of his investigation on the growth of a population of rabbits. Fibonacci multilayer photonic structure can be grown by juxtaposing two building blocks A and B, in such a way that the nth-stage of the superlattice S_N is given iteratively by the rule $S_N = \{S_{N-1}, S_{N-2}\}$ for $N \geq 2$ with $S_0 = \{B\}$ and $S_1 = \{A\}$. The number of layers is given by F_N, where F_N is the Fibonacci number obtained from recursive relation $F_N = F_{N-1} + F_{N-2}$, with $F_0 = F_1 = 1$, and the ratio between the number of building blocks A and the number of building blocks B in the sequence is equal to the golden mean number $\tau = (1 + \sqrt{5})/2$ [30, 31]. This multilayered photonic structure could be also grown by the inflation rule: $A \longrightarrow AB$, $B \longrightarrow A$. Here, A and B layers are considered as the isotropic positive-index materials. We have chosen medium A as fullerene film whose refraction index is $n_A = 2.1$, while medium B is considered to be Te (with $n_B = 4.6$), Ge (with $n_B = 4.2$) and GaAs (with $n_B = 3.6$).

Fullerene (C60) in the form thin film structure is a suitable candidate for the designing the PC structure because alkali-metal doped thin film of fullerene acts as conductor and have almost zero absorption in the wavelength range > 530 nm and near IR region [25]. Also, in this region its dielectric constant has very small dependence on the frequency and can be ignored. Thus being a metallic counter part as well as almost frequency independent dielectric constant and easier fabrication technique it is useful in designing the PC structure [26–29]. The proposed structure gives 100% reflection within a wide range of wavelength in the near IR region and in a narrow portion of visible region of the EM spectrum.

In this paper, we take a certain level of the Fibonacci sequence as a 1D superlattice to calculate the photonic transmission and phase treatment of reflected waves. The analysis has been done by using theoretical model based on the transfer matrix method (TMM). For this purpose, we assume that a

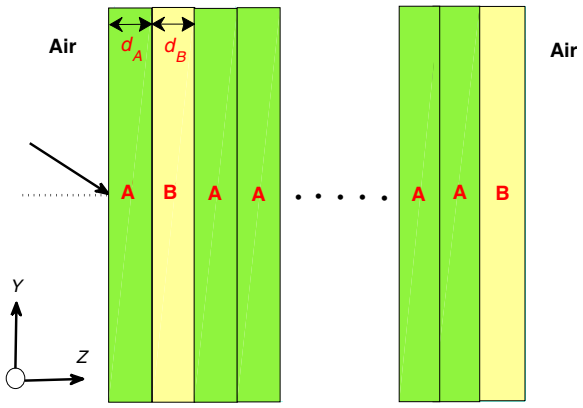

Figure 1. Schematic drawing of the one-dimensional quasiperiodic Fibonacci structure, which is embedded in air. The thicknesses of A and B are supposed to be d_A and d_B, respectively.

plane wave be incident from air with angle θ onto a fractal multilayer structure, as shown in Fig. 1. For TE polarization, the electric field E is assumed in the x direction (the layers are in the x-y plane), and the z direction is normal to the interface of each layer. In general, the electric and magnetic fields at any two positions z and $z + \Delta z$ in the same layer can be related via a transfer matrix [32]

$$M_j(\Delta z, \omega) = \begin{pmatrix} \cos(k_z^j \Delta z) & \frac{i}{q_j}\sin(k_z^j \Delta z) \\ iq_j \sin(k_z^j \Delta z) & \cos(k_z^j \Delta z) \end{pmatrix}, \tag{1}$$

where $k_z^j = (\omega/c)\sqrt{\epsilon_j}\sqrt{\mu_j}\sqrt{1 - \sin^2\theta/\epsilon_j\mu_j}$ is the component of the wave vector along the z axis, c indicates the speed of light in vacuum, $q_j = \sqrt{\epsilon_j}/\sqrt{\mu_j}\sqrt{1 - \sin^2\theta/\epsilon_j\mu_j}$ for TE polarization, and $j = A,\ B$ and $C_{1,2,\ldots}$. The transmission coefficient $t(\omega, \theta)$ can be expressed as

$$t(\omega, \theta) = \frac{2\cos\theta}{(m_{11} + m_{22})\cos\theta + i(m_{12}\cos^2\theta - m_{21})}, \tag{2}$$

Here m_{ij} $(i, j = 1, 2)$ are the matrix elements of $X_N(\omega) = \prod_{j=1}^{N} M_j(d_j, \omega)$ which represents the total transfer matrix connecting the fields at the incidence and exit ends. The treatment for TM wave is similar to that for TE wave.

3. RESULTS AND DISCUSSION

The Fibonacci superlattice discussed in this work, which is embedded in air, is depicted in Fig. 1. The building blocks A and B (organized according to the Fibonacci sequence) are assumed to be fullerene and Te (Ge or GaAs), respectively. In other words, we consider the three different arrangements as fullerene-Te, fullerene-Ge and fullerene-GaAs to fabricate our supposed Fibonacci structure. Here, all materials are taken to be absorption less and isotropic. In numerical computations, the refractive index and thickness of A layers are set to be $n_A = 2.1$ and $d_A = 65\,\text{nm}$, respectively. For B type layers with thickness $d_B = 40\,\text{nm}$, the refractive index of Te, Ge and GaAs materials are taken to be 4.6, 4.2 and 3.6, respectively. Now, by using the transfer matrix method described in the previous section, we investigate the transmission spectra and phase treatment of EM waves in the above mentioned arrangements. For the Fibonacci generation number $N = 9$ (S9), the transmission spectrum and phase treatment of reflected waves in the presented fullerene-Te, fullerene-Ge and fullerene-GaAs Fibonacci superlattices are calculated based on the theoretical model described in the previous section. For the 9th level of the Fibonacci sequence, the number of A-type slabs (N_A) and B-type slabs (N_B) are 34 and 21, respectively.

In Figs. 2–4, we show transmittance spectra of 1D fullerene-Te (see Fig. 2), fullerene-Ge (see Fig. 3), fullerene-GaAs (see Fig. 4) Fibonacci multilayer structures for both TE (see Figs. 2(a)–4(a)) and TM

(see Figs. 2(b)–4(b)) polarizations versus wavelength at different incident angles as 0° (solid line), 30° (dashed line) and 60° (dotted line). It is clear from these figures that in the transmission spectra of all arrangements there is a band gap for both TE and TM waves in the near infrared wavelength region nearly 680 to 950 nm for fullerene-Te arrangement, 670 to 850 nm for fullerene-Ge arrangement and 650 to 750 nm for fullerene-GaAs arrangement. As shown in Fig. 2, for both TE and TM polarizations

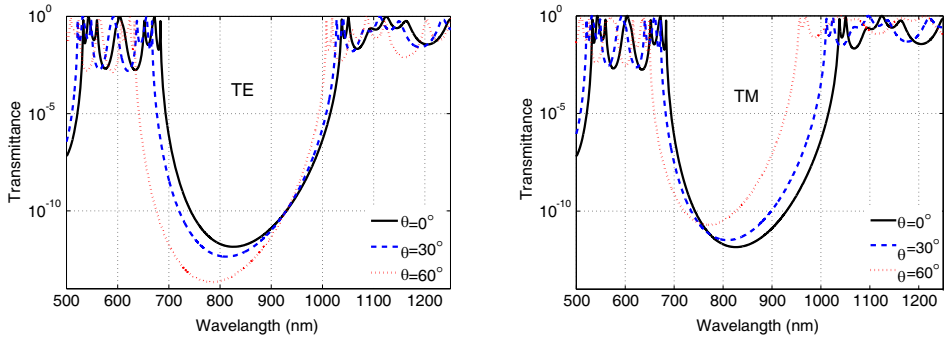

Figure 2. The transmissions spectra of S9 fullerene-Te Fibonacci quasiperiodic structure for (a) TE and (b) TM waves at different incident angles as 0 (solid line), 30 (dashed line) and 60 (dotted line). Structure parameters are $d_A = 65\,\text{nm}$, $d_B = 40\,\text{nm}$, $n_A = 2.1\,\text{mm}$ and $n_B = 4.6$.

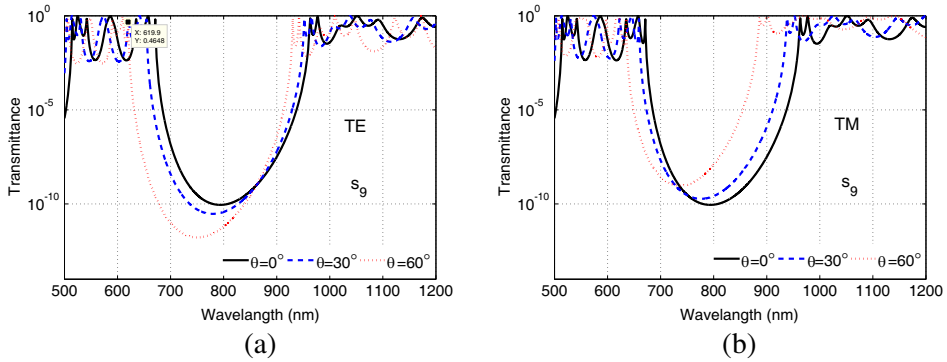

Figure 3. The transmissions spectra of S9 fullerene-Ge Fibonacci quasiperiodic structure for (a) TE and (b) TM waves at different incident angles as 0 (solid line), 30 (dashed line) and 60 (dotted line). The physical parameters are the same as those of Fig. 2.

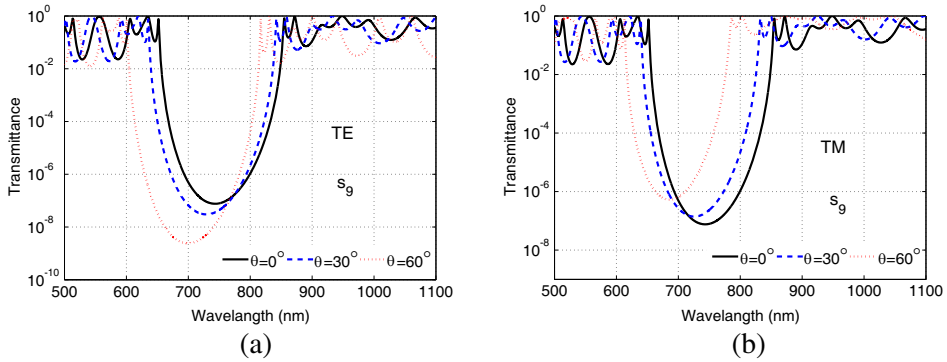

Figure 4. The transmissions spectra of S9 fullerene-GaAs Fibonacci quasiperiodic structure for (a) TE and (b) TM waves at different incident angles as 0 (solid line), 30 (dashed line) and 60 (dotted line). The physical parameters are the same as those of Fig. 2.

as the incident angle increases the higher and lower edges of the gap shift to higher frequencies. An extensive review that emphasizes the physical phenomenon's, which generate these results, can be found in [31].

By considering the same physical parameters as those of Fig. 2, in the fullerene-Te arrangement the photonic spectra of the three other successive generations are investigated at different incident angles and for both TE (see Fig. 5) and TM (see Fig. 6) waves. For this purpose, the three Fibonacci order as S_{10} (solid line), S_{11} (dashed line) and S_{12} (dotted line) are considered. It is clearly shown in Figs. 5 and 6 that for both TE and TM polarizations by increasing order of the Fibonacci structure, the transmittance band remains invariant and the edges of the transmittance band become much sharper. In fact, the transmittance band can occur in all higher-order Fibonacci structures, i.e., it is insensitive to the order of the Fibonacci sequence. For simplicity, others are not given in this paper. The same results are obtained for the fullerene-Ge and fullerene-GaAs arrangements.

The essential aim of this work is the investigation of the properties of phase shifts upon reflection (or transmission) from 1D Fibonacci multilayer structure containing nano-fullerene thin films. So, we study the phase shift ϕ of TE and TM waves in the stop band of supposed structure by the transfer matrix method. The phase shift of EM wave within the band gap of 1D PC comes from the total effect of the reflections and refractions on each interface according to Fresnels law. We calculate the dependence of the phase shift ϕ of reflected waves of TE and TM modes on the wavelength and incident angle in the S9 structure. The physical parameters are the same as those of Fig. 2. The results are shown in Figs. 7–9. In these figures, the three incident angles such as 0° (solid line), 45° (dashed line) and 89° (dotted line) are supposed. From Figs. 7–9, we conclude that for both TE (see solid lines in Figs. 7–9) and TM (see dashed lines in Figs. 7–9) polarizations as the incident angle and wavelength increase, the phase shift of TE wave (ϕ_{TE}) in the stop band decrease (shift downward), while that of TM wave (ϕ_{TM}) in the stop band increase (shift upward). In the stop band at incident angle 89° (dotted line) the curve of ϕ_{TE} versus wavelength becomes bottom-flat, i.e., $\phi = -\pi/2$, but for TM wave we have top-flat case, i.e., $\phi = \pi/2$. So, the phase shift treatment of TM and TE modes is just opposite phase in the whole gap.

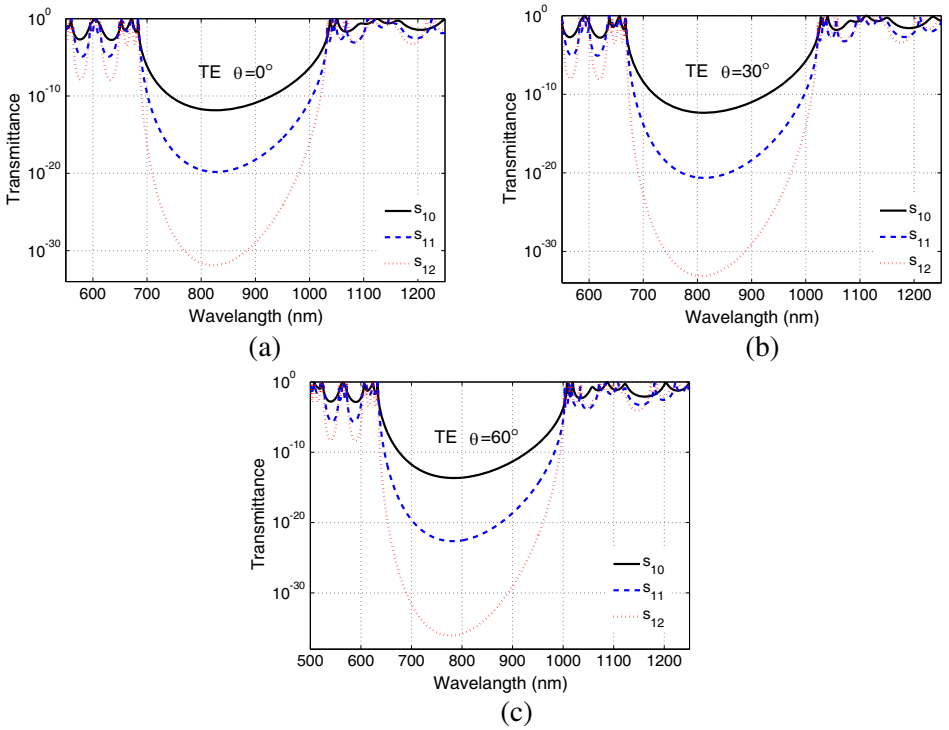

Figure 5. The transmission spectra for TE wave in the fullerene-Te arrangement the three Fibonacci order as S_{10} (solid line), S_{11} (dashed line) and S_{12} (dotted line) at different incident angles (a) 0, (b) 30 and (c) 60. The physical parameters are the same as those of Fig. 2.

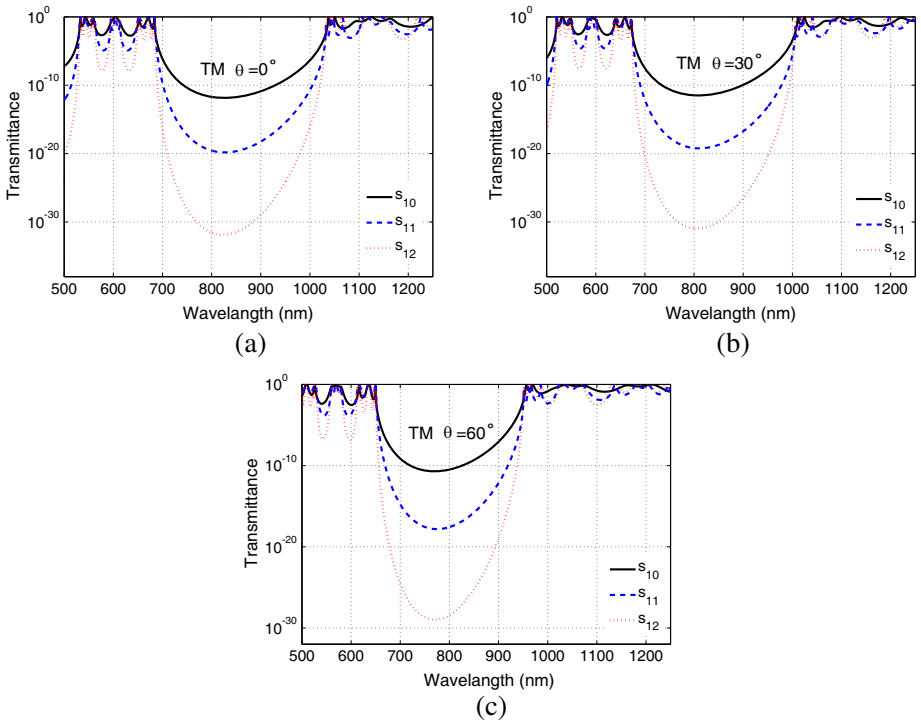

Figure 6. The transmission spectra for TM wave in the fullerene-Te arrangement for the three Fibonacci order as S_{10} (solid line), S_{11} (dashed line) and S_{12} (dotted line) at different incident angles as (a) 0, (b) 30 and (c) 60. The physical parameters are the same as those of Fig. 2.

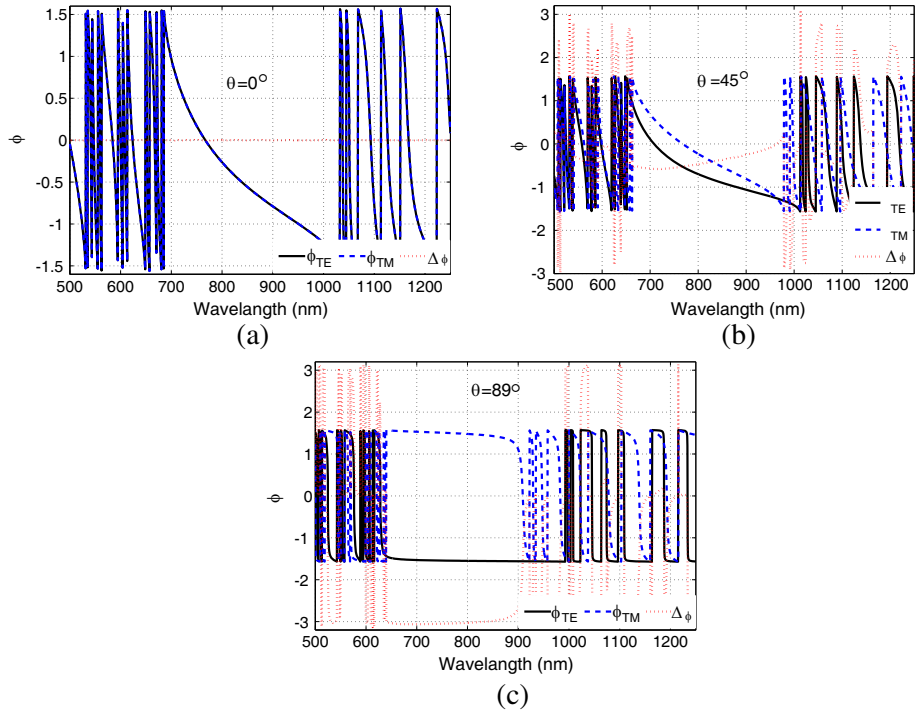

Figure 7. The reflection phase shift for TE and TM waves in the fullerene-Te arrangement versus wavelength at different incident angles as as (a) 0, (b) 30 and (c) 89. The physical parameters are the same as those of Fig. 2.

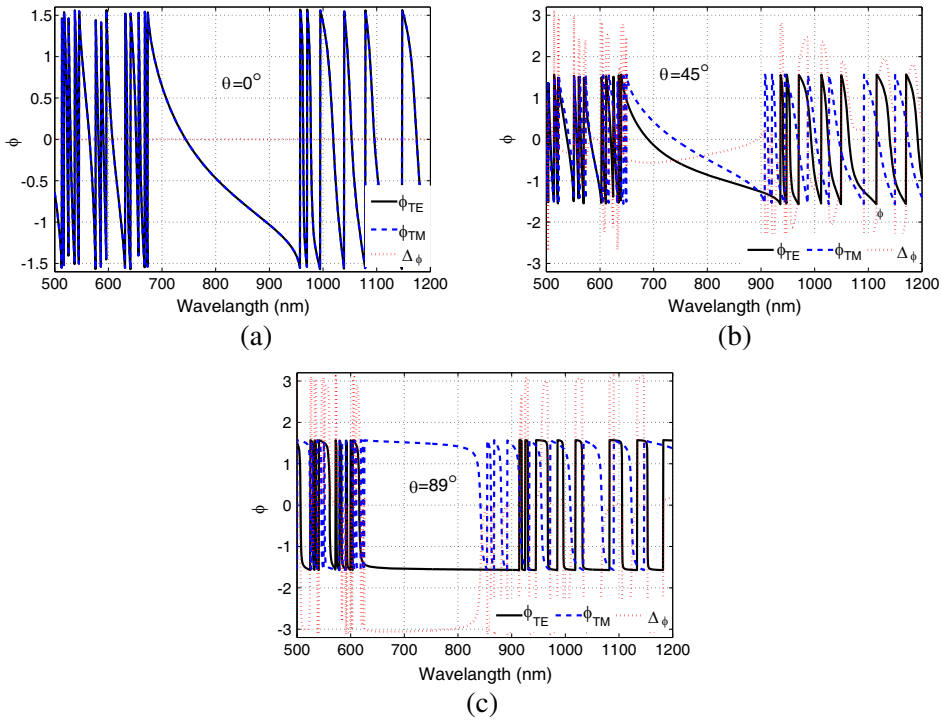

Figure 8. The reflection phase shift for TE and TM waves in the fullerene-Ge arrangement versus wavelength at different incident angles as as (a) 0, (b) 30 and (c) 89. The physical parameters are the same as those of Fig. 2.

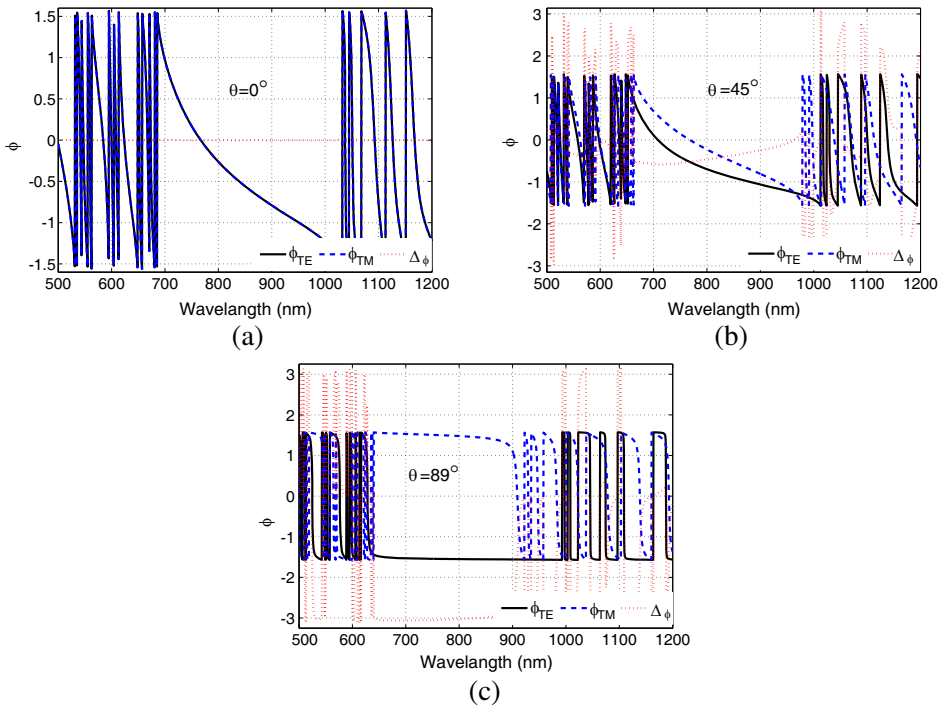

Figure 9. The reflection phase shift for TE and TM waves in the fullerene-GaAs arrangement versus wavelength at different incident angles as as (a) 0, (b) 30 and (c) 89. The physical parameters are the same as those of Fig. 2.

This property is very useful in phase compensators, because it provides two light waves with opposite phase in much wide frequency range. Moreover, it is clearly seen that in the stop band, the phase shift changes smoothly as the frequency changes, while in the pass band, the phase shift changes sharply. We also calculate the difference between the phase shift of TE and that of TM reflected wave versus wavelength at different incident angles (see dotted lines in Figs. 7–9). In these figures, it is clearly seen that at normal incidence the phase difference $\Delta\phi$ between TE and TM waves is equal zero in the both stop and pass bands, i.e., in this structure a linear polarized incident wave will not undergo any phase delay. At oblique incident angles, when θ is varied from 0° to 89°, the corresponding $\Delta\phi = \phi_{TE} - \phi_{TM}$ of two polarizations gradually increases until it reaches to π (or $-\pi$) (see Figs. 7(c)–9(c)). Meanwhile, at both the edges of the gap the reflection phase difference keeps zero in spite of the change of incident angle. It is worthy of noting that the thickness of each layer of structure is less than the wavelength of the incident wave. The thickness of the whole supposed structure is about 3λ. Therefore, based on these studies, our supposed structure provides a convenient way to design very compact wave plates, phase retarders, phase-sensitive interferometry, phase compensators with broad spectral band width and phase modulators.

In Figs. 10–12, which are interesting figures, for all arrangements we obtain a stop band which is common and identical for all of the incident angles and polarizations. We can call this stop band as semi-omnidirectional band gap. For this purpose, in Figs. 10, 11 and 12 we plot the difference between the phase shift of TE and that of TM reflected wave as a function of the incident angle in the stop band for the lower edge wavelength (see Figs. 10(a), 11(a) and 12(a)), central wavelength (see Figs. 10(b), 11(b) and 12(b)) and the higher edge wavelength (see Figs. 10(c), 11(c) and 12(c)). The lower band edge, central and the higher band edge wavelengths of fullerene-Te arrangement are $\lambda = 674\,\text{nm}$, $\lambda = 764\,\text{nm}$ and $\lambda = 854\,\text{nm}$, respectively, while those in the fullerene-Ge arrangement are $\lambda = 674\,\text{nm}$, $\lambda = 764\,\text{nm}$ and $\lambda = 854\,\text{nm}$, respectively. Also, in the fullerene-GaAs arrangement, they are $\lambda = 655\,\text{nm}$, $\lambda = 705\,\text{nm}$ and $\lambda = 755\,\text{nm}$, respectively. In the Figs. 10–12 solid, dashed and dotted

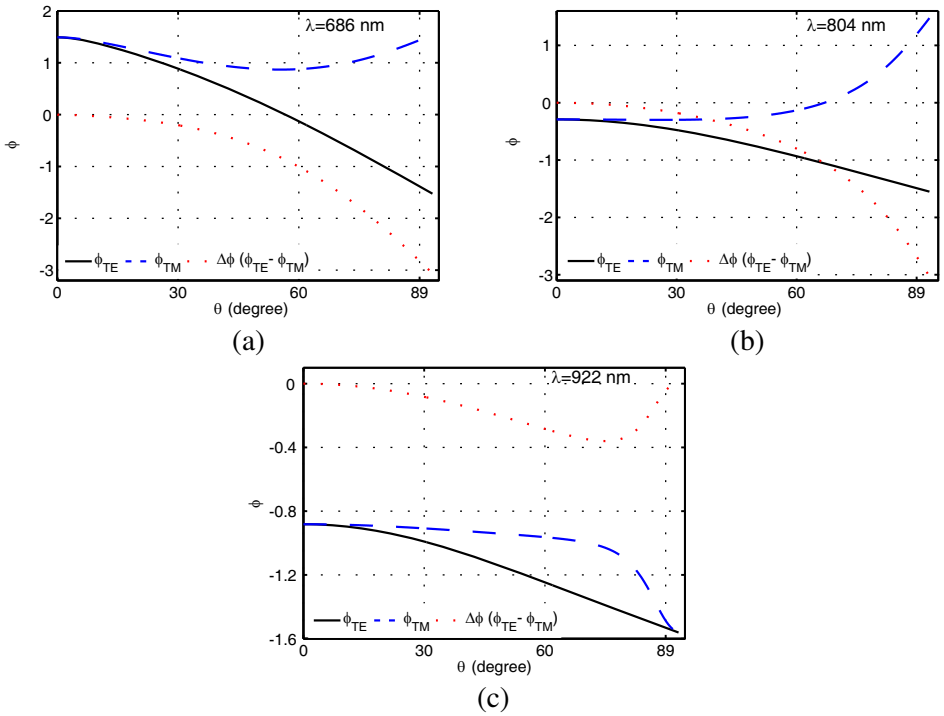

Figure 10. The difference between the phase shift for TE and of TM waves in the fullerene-Te arrangement as a function of the incident angle in the stop band at the lower edge wavelength, (a) $\lambda = 686\,\text{nm}$, central wavelength, (b) $\lambda = 804\,\text{nm}$ and the higher edge wavelength, (c) $\lambda = 922\,\text{nm}$. The physical parameters are the same as those of Fig. 2.

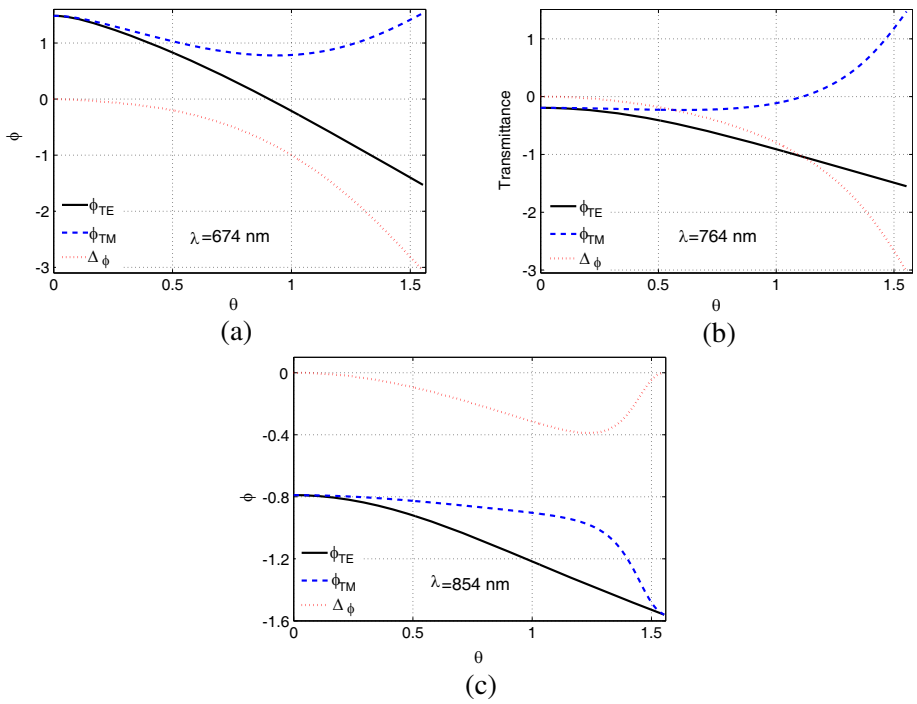

Figure 11. The difference between the phase shift for TE and of TM waves in the fullerene-Ge arrangement as a function of the incident angle in the stop band at the lower edge wavelength (a) $\lambda = 674\,\text{nm}$, central wavelength, (b) $\lambda = 764\,\text{nm}$ and the higher edge wavelength, (c) $\lambda = 854\,\text{nm}$. The physical parameters are the same as those of Fig. 2.

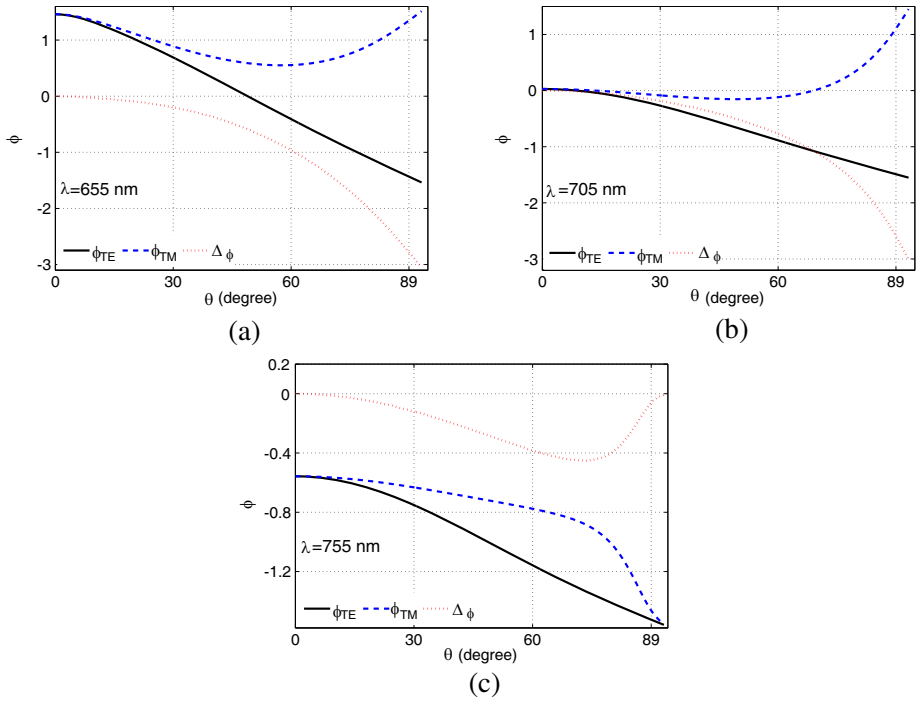

Figure 12. The difference between the phase shift for TE and of TM waves in the fullerene-GaAs arrangement as a function of the incident angle in the stop band at the lower edge wavelength (a) $\lambda = 655\,\text{nm}$, central wavelength, (b) $\lambda = 705\,\text{nm}$ and the higher edge wavelength, (c) $\lambda = 755\,\text{nm}$. The physical parameters are the same as those of Fig. 2.

lines are related to the ϕ_{TE}, ϕ_{TM} and $\Delta\phi = \phi_{TE} - \phi_{TM}$, respectively. From our calculation, it is found that $\Delta\phi$ changes more slowly within the stop band as the wavelength and incident angle change. $\Delta\phi$ values for example in the Fig. 10, at the lower band edge and for the incident angles 30° and 60° are -0.2 and -1, respectively, while those at the higher stop band edge are -0.08 and -0.28, respectively. So, for a wavelength within the stop band we can adjust the value of $\Delta\phi$ by changing the incident angle. Also, for the incident angles near 0° the difference of the phase shift of TE and TM waves is nearly 0, i.e, insensitive to the incident angle.

4. CONCLUSIONS

In summary, the properties of the phase shift of wave reflected from one-dimensional photonic crystals containing nano-scale fullerene and Te (Ge or GaAs) thin films as fullerene-Te, fullerene-Ge and fullerene-GaAs arrangements have been investigated by transfer matrix method. For the three arrangements, it is found that there is a band gap which is insensitive to the order of the Fibonacci sequence. Also, as the incident angle increases, the reflection phase shift of TE wave decreases, while that of TM wave increases. The phase shifts of both polarized waves in the stop band vary smoothly while in the pass band change sharply as the wavelength and incident angle change. Moreover, we obtained a stop band in the wavelength range from 686 to 922 nm which is common and identical for all of the incident angles and polarizations. We called this stop band as semi-omnidirectional band gap. Based on our results, the supposed structure provides a convenient way to design very compact wave plates, phase retarders, phase-sensitive interferometry, phase compensators with broad spectral band width and phase modulators.

REFERENCES

1. Shechtman, D., I. Blech, D. Gratias, and J. W. Cahn, "Metallic phase with long-range orientational order and no translational symmetry," *Phys. Rev. Lett.*, Vol. 53, 1951, 1984.
2. Janot, C., *Quasicrystals*, Clarendon Press, Oxford, 1994.
3. Sheng, P., *Introduction to Wave Scattering, Localization and Mesoscopic Phenomena*, Academic Press, New York, 1995.
4. Zoorob, M. E., M. D. Charlton, G. J. Parker, and M. C. Netti, "Complete photonic bandgaps in 12-fold symmetric quasicrystals," *Nature*, Vol. 404, 740, 2000.
5. Albuquerque, E. L. and M. G. Cottam, *Polaritons in Periodic and Quasiperiodic Structures*, Elsevier, Amsterdam, 2004.
6. Luck, J. M., C. Godreche, A. Janner, and T. Janssen, "The nature of the atomic surfaces of quasiperiodic self-similar structures," *J. Phys. A*, Vol. 26, 1951, 1993.
7. Boyd, R. W., *Nonlinear Optics*, Academic Press, Boston, 2008.
8. Zhu, S., Y. Y. Zhu, and N. B. Ming, "Quasi-phase-matched third-harmonic generation in a quasi-periodic optical superlattice," *Science*, Vol. 278, 843, 1997.
9. Macia, E., "Optical applications of fibonacci dielectric multilayers," *Ferroelectrics*, Vol. 250, 401, 2001.
10. Aissaoui, M., J. Zaghdoudi, M. Kanzari, and B. Rezig, "Optical properties of the quasi-periodic one-dimensional generalized multilayer Fibonacci structures," *Progress In Electromagnetics Research*, Vol. 59, 69–83, 2006.
11. Cojocaru, E., "Omnidirectional reflection from finite periodic and fibonacci quasi-periodic multilayers of alternating isotropic and birefringent thin films," *Appl. Opt.*, Vol. 41, 747, 2002.
12. Zhang, H., S. Liu, X. Kong, B. Bian, and Y. Dai, "Omnidirectional photonic band gaps enlarged by Fibonacci quasi-periodic one-dimensional ternary superconductor photonic crystals," *Solid State Commun.*, Vol. 152, 2113, 2012.
13. Zhang, H., J. Zhen, and W. He, "Omnidirectional photonic band gaps enhanced by Fibonacci quasiperiodic one-dimensional ternary plasma photonic crystals," *Optik*, Vol. 124, 4182, 2013.

14. Kratschmer, W., L. D. Lamb, K. Fostiropoulos, and D. R. Huffman, "Solid C60: A new form of carbon," *Nature*, Vol. 347, 354–358, 1990.
15. Rosseinsky, M. J., A. P. Ramirez, S. H. Glarum, D. W. Murphy, R. C. Haddon, A. F. Hebard, T. T. M. Palstra, A. R. Kortan, S. M. Zahurak, and A. V. Makhija, "Superconductivity at 28 K in RbxC60," *Phys. Rev. Lett.*, Vol. 66, 2830–2832, 1991.
16. Taigaki, K., I. Hirosawa, T. W. Ebbsen, J. Mizuki, Y. Shimakawa, Y. Kubo, J. S. Tsai, and S. Kuroshima, "Superconductivity in sodium and lithium containing alkali-metal fullerides," *Nature*, Vol. 356, 419–421, 1992.
17. Hiromichi, K. H., E. Y. Yasushi, A. Y. Yohji, K. K. Koichi, H. T. Takaaki, and Y. S. Shigeo, "Dielectric constants of C60 and C70 thin films," *J. Phys. Chem. Solids*, Vol. 58, 1923, 1997.
18. Haddon, R. C., "Conducting films of C60 and C70 by alkali metal doping," *Nature*, Vol. 350, 320–322, 1991.
19. Xiong, Z. W., F. Jiang, and X. R. Chen, "Structural and optical properties of fullerene-like amorphous carbon with embedded dual-metal nanoparticles," *J. of Alloys and Compounds*, Vol. 574, 13, 2013.
20. Akkurt, F., "Laser induced electro-optical characterization of anthraquinone dye and fullerene C60 doped guest-host liquid crystal systems," *J. of Molecular Liquids*, Vol. 194, 241, 2014.
21. Makarova, T. L., V. G. Melekhin, I. T. Serenkov, V. I. Sakharov, I. B. Zakharova, and V. E. Gasumyants, "Optical and electrical properties of C60Tex films," *Phys. the Solid State*, Vol. 43, 1393, 2001.
22. Xu, H., D. M. Chen, and W. N. Creager, "C60-induced reconstruction of the Ge(111) surface," *Phys. Rev. B*, Vol. 50, 8454, 1994.
23. Xu, Q., Y. Ling, T. Ogino, et al., "C60 single crystal films on GaAs (001) surfaces," *Thin Solid Films*, Vol. 281, 618, 1996.
24. Giudice, E., E. Magnano, S. Rusponi, et al., "Morphology of C60 thin films grown on Ag (001)," *Surf. Sci. Lett.*, Vol. 405, 561, 1998.
25. Peide, H., X. Bingshe, L. Jian, L. Xuguang, and H. BaoBand, "Band gaps of two-dimensional photonic crystal structure using fullerene films," *Physica E*, Vol. 25, 29, 2004.
26. Bingshe, X., H. Peide, L. Jian, L. Xuguang, and C. Mingwei, "Optical properties in 2D photonic crystal structure using fullerene and azafullerene thin films," *Opt. Commun.*, Vol. 250, 120, 2005.
27. Bingshe, X., H. Peide, L. Jian, B. Huiqiang, C. Mingwei, and H. Ichinose, "Theoretical investigation of the reflectivity of fullerene-(C60, C70)/AlN multilayers in UV region," *Solid State Commun.*, Vol. 133, 353, 2005.
28. Won-Chun, O. and K. Weon-Bae, "Characterization and photonic properties for the Pt-fullerene/TiO2 composites derived from titanium (IV) n-butoxide and C60," *J. of Industrial and Engineering Chemistry*, Vol. 15, 791–797, 2009.
29. Wu, C., "Transmission and reflection in a periodic superconductor/dielectric film multilayer structure," *J. Electromagn. Waves Appl.*, Vol. 19, 1991–1996, 2006.
30. Merlin, R., K. Bajema, R. Clarke, and F. Juang, "Quasiperiodic GaAs-AlAs Heterostructures," *Phys. Rev. Lett.*, Vol. 55, 1768, 1985.
31. Albuquerque, E. L. and M. G. Cottam, "Theory of elementary excitations in quasiperiodic structure," *Physics Reports*, Vol. 376, 225–237, 2003.
32. Yeh, P., *Optical Waves in Layered Media*, John Wiley and Sons, New York, 1988.